

Surface-Reconstruction-Switched Adsorbate Photofragmentation Dynamics

Nicholas Camillone III,^{1,*} Khalid A. Khan,¹ Jory A. Yarmoff,² and Richard M. Osgood, Jr.¹

¹*Columbia Radiation Laboratory, Columbia University, New York, New York 10027*

²*Department of Physics, University of California–Riverside, Riverside, California 92521*

(Received 14 September 2000; published 11 July 2001)

Energy-resolved angular distributions of neutral fragments ejected during photoinduced electron transfer reaction of CH_3Br on $\text{GaAs}(100)$ exhibit three distinct methyl-radical ejection channels. These undergo marked changes when the termination is switched from the Ga-rich $c(8 \times 2)$ to the As-rich $c(2 \times 8)$. Our observations are consistent with a strong adsorption-site dependence of the dynamics.

DOI: 10.1103/PhysRevLett.87.056101

PACS numbers: 82.65.+r, 68.43.Fg, 79.20.La, 82.30.Fi

Anisotropies in the angular distributions of fragments ejected from single crystal surfaces during photon- and electron-induced molecular fragmentation are important to understanding radical-surface and radical-adsorbate interaction dynamics. In the case of photoinduced dissociative electron attachment, trajectories of neutral product fragments reflect the initial adsorbate orientation, when their separation occurs on a strongly repulsive intramolecular potential energy surface (PES). Surface sites have been identified that bind adsorbates in a narrow range of orientations, such that, when the molecule is excited to a dissociative state, product fragments exit with narrow angular and energy distributions [1]. The chemistry between such fragments and coadsorbates has been termed surface-aligned photoreaction (SAP) [2] and is relevant to catalysis, atmospheric chemistry, and nanofabrication [3].

Understanding and controlling SAPs requires identifying the dependence of the fragmentation dynamics upon the structure and chemical nature of the adsorption site. While there have been observations of fragmentation of molecules oriented on single-crystal surfaces, it has not been possible to compare the same dissociation event for two distinct sites on closely related surfaces. Such an experiment would allow for systematic examination of the effects of surface structure and chemistry. The (100) facet of III-V semiconductors presents a unique opportunity for such a study on a substrate with well-characterized structurally related, yet chemically distinct terminations.

In this Letter, we describe experiments that show for the first time that switching the surface reconstruction of $\text{GaAs}(100)$ from the Ga-rich $c(8 \times 2)$ to the As-rich $c(2 \times 8)$ leads to clear, reproducible changes in the angular distributions of fragments generated by photoinitiated dissociative electron attachment to adsorbates. Our mass- and energy-resolved angular-distribution measurements of the photoinduced chemistry of $\text{CH}_3\text{Br}/\text{GaAs}(100)$ reveal dramatic differences among the hyperthermal methyl-radical ejection channels that reflect the preirradiation orientations of the adsorbate and are consistent with molecular adsorption at distinct surface sites.

We chose the (100) surface of GaAs because its reconstruction can be switched *in situ* [4]. The most widely

accepted structures for the Ga- and As-rich surfaces [see Figs. 1(a) and 1(b)] are the $\beta 2(2 \times 4)$ and $\beta 2(4 \times 2)$, which are chemical “mirror images” of each other: The lattice of one can be constructed from the other by switching As for Ga atoms, and vice versa, and rotating the lattice by 90° [5]. The $2 \times$ periodicity arises from the formation of dimers, while the $8 \times$ periodicity results from a patterned arrangement of missing dimers. Note that recent literature has suggested a different possible structure for the Ga-rich surface [6], but we restrict our discussion to the $\beta 2$ structures and note that some adjustments may need to be made as this structure continues to be refined. The (100) surface also has similarities in local geometrical and

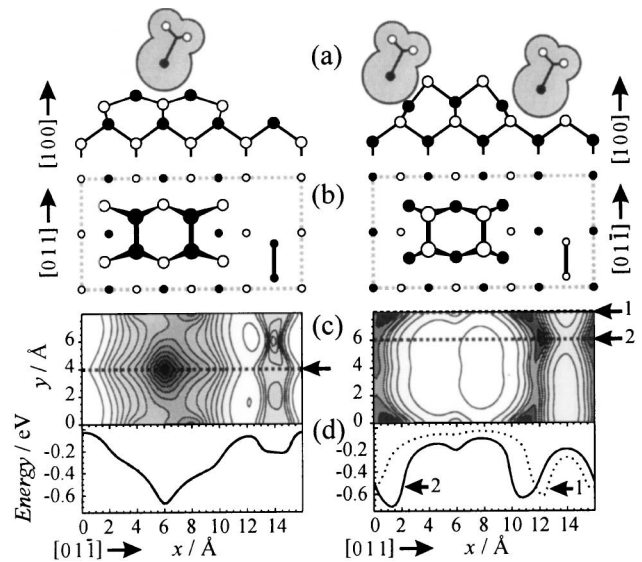


FIG. 1. Side (a) and top (b) views of CH_3Br adsorbed on the (4×2) subcell of the Ga-rich $c(8 \times 2)$, left, and the (2×4) subcell of the As-rich $c(2 \times 8)$ reconstructions of $\text{GaAs}(100)$. Solid circles represent Ga and open circles As. In the top view, the larger the circle, the closer the represented atom is to the surface. In (b), bold vertical lines represent dimer bonds. The Ga and As atomic positions were taken from *ab initio* calculations for the $\beta 2(2 \times 4)$ and $\beta 2(4 \times 2)$ structures [5a,5b]. Contour plots of the corresponding minimum potential energy surfaces along with cuts through that surface along the indicated dashed lines calculated for CH_3Br are shown in (c) and (d).

electronic structure with the (110) surface [7], a substrate used in prior investigations of adsorbate orientation and photoinduced electron-transfer chemical dynamics [1,8–10]. *Ab initio* calculations indicate that the CH_3Br is held at the (110) surface due to electrostatic forces and the affinity of the Br lone pairs for the empty Ga dangling bonds. Their orientation is driven by alignment of the molecular dipole with surface dipoles [10], and a single adsorption site is identified. By comparison, the (100) surface is substantially more complex and presents a rich variety of adsorption sites.

The experiments were performed in a UHV system (base pressure $\sim 2 \times 10^{-10}$ torr) [8], equipped with a low energy electron diffraction (LEED) apparatus, a quadrupole mass spectrometer (QMS), a solid-state electrochemical iodine source [4,11], and an effusive-beam gas doser. The (100) surface of the GaAs crystals (Si-doped, *n*-type, $\sim 5.5 \times 10^{-17} \text{ cm}^{-3}$) was prepared using the following protocol [4]: Repeated cycles of sputtering with 1 keV Ar^+ ions and 840 K anneals resulted in formation of the Ga-rich $c(8 \times 2)$ surface, as confirmed by LEED measurements. From the Ga-rich, the As-rich surface was prepared by exposure to a molecular beam of I_2 from the electrochemical cell. Annealing the iodine-covered surface at 750 K generated the As-rich surface, as confirmed by observation of a $c(2 \times 8)$ LEED pattern.

The surfaces were cooled to 90 K and dosed with sufficient CH_3Br to produce a monolayer, as characterized by temperature programmed desorption (TPD) measurements. A pulsed excimer laser ($\lambda = 193, 248, \text{ or } 351 \text{ nm}$) initiated molecular fragmentation. Mass- and energy-resolved angular distributions were measured with the QMS in time-of-flight (TOF) mode: During irradiation, ejected particles were monitored as a function of time of arrival at the detector. Variations in the emission angle were determined by rotating the crystal. In this Letter, plots of ejected CH_3 flux vs detection angle are normalized to present the measured flux per *adsorbed* photon (calculated using the Fresnel equations) per unit area probed.

Energy-resolved photofragment angular distributions were recorded in the $[01\bar{1}]$ and the $[011]$ directions for both terminations. UV exposure of the CH_3Br monolayers causes C—Br bond cleavage, resulting in the formation of a surface gallium bromide species and energetic CH_3 radicals [1a,1b]. The TOF spectra from the (100) surfaces are more sensitive to laser exposure than those from the (110) surface due to a photochemical modification of the surface stoichiometry [12], which was avoided by using pristine surfaces.

Velocity distributions, measured from $+70^\circ$ to -70° along the $[01\bar{1}]$ and $[011]$ directions for the As- and Ga-rich surfaces, exhibited angular dependencies revealing a complexity in the fragmentation dynamics distinct from the simple distributions measured on GaAs(110) [8a]. Figure 2 illustrates this angular dependence, showing three observed CH_3 ejection channels. The data contain important simplifying features. First, all the measured

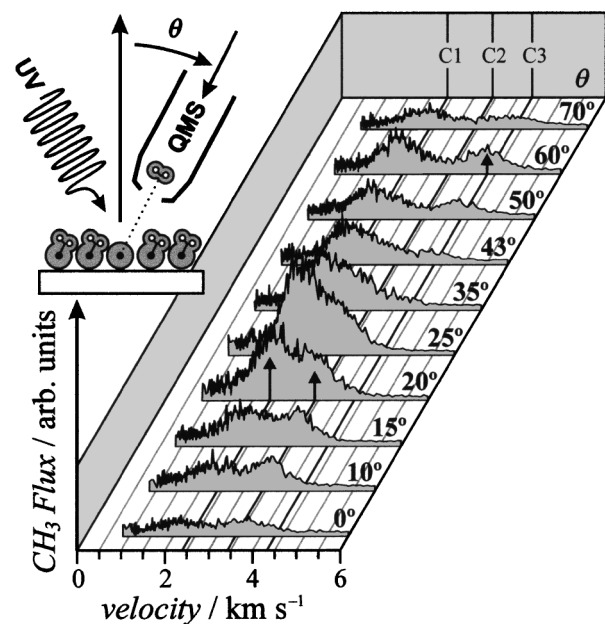


FIG. 2. The angular dependence of the CH_3 velocity distributions measured along the $[011]$ azimuth for the As-rich surface during irradiation at 351 nm with 0.3 mJ/cm^2 . Three distinct velocity distributions, marked C1, C2, and C3, are observed (average kinetic energies: 0.47, 0.93, and 1.4 eV, respectively).

angular distributions were found to be symmetric about the surface normal, within experimental uncertainty ($\sim 20\%$). This result is distinct from GaAs(110), where asymmetry in surface structure is clearly reflected in the angular distributions [1a,8a]. For the (100) case, the $[100]$ - $[01\bar{1}]$ and $[100]$ - $[011]$ planes are mirror planes of symmetry, and the symmetry in the angular distributions is expected. A second simplifying feature is that all the CH_3 velocity distributions consist of linear combinations of distributions that, within $\sim \pm 20\%$, cluster about three distinct values: ~ 0.5 , ~ 1.0 , and $\sim 1.8 \text{ eV}$, designated as channels C1, C2, and C3, respectively. The measured angular distributions were separated into their constituent energy-resolved components by fitting the TOF data with modified Maxwell-Boltzmann (MMB) velocity distributions [13,14]. The results are displayed in Fig. 3 as a function of polar angle in four separate panels. The top panels contain measurements made on the Ga-rich surface; the bottom those on the As-rich. The data on the left-hand side were taken along the $[01\bar{1}]$ azimuth [i.e., along the $8\times$ and $2\times$ directions of the Ga- and As-rich surface, respectively]; those on the right-hand side were taken along the $[011]$ azimuth [i.e., along the $2\times$ and $8\times$ directions of the Ga- and As-rich surface, respectively]. Since the data were symmetric about the surface normal, we show only data for one side of the normal. Measurements taken at all wavelengths along both azimuths revealed that the energy-resolved angular distributions vary only slightly with photon energy.

The data for the As-rich surface in Fig. 3(d) show that, in the $[011]$ direction, two energetic channels are resolved.

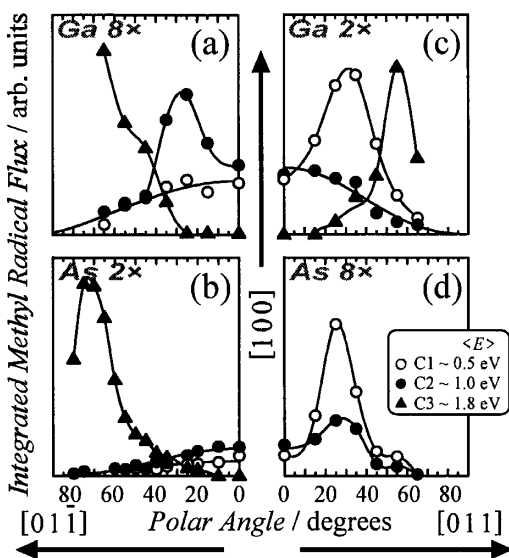


FIG. 3. Results of TOF angular distribution measurements for the three CH_3 ejection channels for both the Ga-rich [(a), (c)] and As-rich [(b), (d)] taken along the two principal crystallographic directions.

The slower channel, characterized by an average CH_3 kinetic energy, $\langle E \rangle$, of 0.49 eV (designated C1) is more intense and sharp ($\text{FWHM} \cong 20^\circ$) than the faster channel, $\langle E \rangle = 0.93$ eV (C2, $\text{FWHM} \cong 34^\circ$). The two lobes are both centered at $\sim 28^\circ$. The angular distribution observed in the $[01\bar{1}]$ direction [Fig. 3(b)] is distinct from that along the $[011]$: here, the CH_3 flux is concentrated at large detection angles. Fits of the TOF spectra show the presence of C1 and C2; however, their angular distributions contain considerably less flux than observed along the $[011]$. We believe this is due to the librational motion and finite width in the preirradiation orientational distribution of the adsorbate resulting in the extension of C1 and C2 perpendicular to their native $[011]$ direction. The majority of the flux detected in the $[01\bar{1}]$ is well fit by a third MMB component characterized by an $\langle E \rangle = 1.63$ eV and is peaked at $\sim 73^\circ$ with an estimated FWHM of $\sim 21^\circ$.

Figures 3(a) and 3(c) show that the *angular* distributions for fragments ejected from the Ga-rich surface are dramatically different from those for the As-rich. Nevertheless, the data again show three distinct *velocity* distributions, also designated C1, C2, and C3. The angular distribution of C1 ($\langle E \rangle = 0.35$ eV) is similar to that found for the As-rich surface, although somewhat broader ($\text{FWHM} \cong 33^\circ$) and slightly slower. The intensity of the “tail” along $[01\bar{1}]$, relative to the lobe in the $[011]$ direction, is also significantly larger than for C1 on the As-rich surface. The angular distribution of C2 for the Ga-rich surface is dramatically different from that of the analogous channel for the As-rich. Though its shape is nearly identical, the C2 feature has switched from peaking along the $[011]$ direction (as observed for the As-rich surface) and now is found to peak at $\sim 27^\circ$ along the $[01\bar{1}]$ direction. C3 is also strongly affected by switching the reconstruction. Instead

of appearing only along the $[01\bar{1}]$ azimuth, C3 is now observed along both the $[01\bar{1}]$ and the $[011]$.

It is a striking result that the products are ejected with a variety of characteristic kinetic energies, each with distinct surface-reconstruction-dependent angular distributions. The most obvious interpretation is that the variations in angular distributions of the fragments reflect differing molecular orientations on the two reconstructions. As an initial step in interpreting our observations, we performed adsorption site modeling studies using simple model molecule-surface interactions such as those used in molecular dynamics simulations. Our purpose is to identify, under the constraint of the orientations indicated by the experiment, plausible sites at which the molecule might adsorb. As we will show, the calculations bolster the intuitive interpretation by demonstrating the plausibility of multiple adsorption sites with very similar binding energies. Our model includes molecular dipole-surface charge, surface charge-induced molecular dipole, and molecular dipole-induced surface dipole interactions, as well as Lennard-Jones terms. The substrate atom coordinates were taken from Ref. [5b]. For each of the molecular orientations suggested by our experiment, the model shows sites with binding energies of roughly 0.6 eV, in general agreement with those measured by TPD [12]. The model was tested for $\text{CH}_3\text{Br}/\text{GaAs}(110)$ and found to be reasonably consistent with binding energies and orientations calculated in a previous rigorous *ab initio* study [10]. Nevertheless, this calculation is only suggestive and intended to demonstrate that it is reasonable to attribute the differing fragment energy and angular distributions to molecules in different sites with different orientations. Clearly, a full explanation will require a more rigorous *ab initio* calculation involving the large $c(8 \times 2)$ surface unit mesh.

In our calculations, the molecular orientations were fixed at the angles suggested by our angular distribution measurements, and the height of the molecule above the surface was varied at a given (x, y) in order to find the minimum in the molecule-surface PES. In Fig. 1(c), the values of the minima are plotted as a function of position over the 4×2 subcell for a CH_3Br with its Br end closest to the surface and the molecular axis canted 27° and 28° from the surface normal along the x axis for the Ga- and As-rich surfaces, respectively. The x axis corresponds to the $4 \times$ direction, and $(x, y) = (0, 0)$ Å corresponds to the lower left-hand corner of the unit meshes in panel 1(b). The most obvious feature in the calculations is the reverse “contrast”: on the Ga-rich surface the energy minimum is located at $\sim (6, 4)$ Å, near the center of the Ga-dimer nanoterrace, whereas, on the As-rich surface, the nanoterrace is a region of high potential energy, and the molecules clearly prefer to sit in the trenches which run along the $4 \times$ direction.

The As-rich surface most closely parallels the (110) surface since both have negatively charged surface As atoms located at higher elevations relative to neighboring

positively charged surface Ga atoms. Thus, it is anticipated that the adsorption geometries on the As-(100) surface would be similar to those on the (110) surface. The calculation identifies a minimum at just such a site at $\sim(1.3, 0)$ Å. Another minimum is found at $\sim(12, 6)$ Å, which is only ~ 0.1 eV less tightly bound. Thus, multiple adsorption sites of similar binding energies appear likely and may explain the origins of channels C1 and C2; CH₃ radicals ejected with similar angular distributions but different kinetic energies. In addition, calculations with the CH₃Br tilted at 73° along the *y* axis (results not shown) identify a minimum corresponding to molecules lying along the large trenches parallel to the 2× direction corresponding to the C3 feature.

Assuming the $\beta 2(4 \times 2)$ structure for the Ga-rich surface, the strong preference for adsorption atop the nanoterraces is due to the strong interaction between the negatively charged Br end of the molecule and the positively charged surface Ga atoms. Our calculations suggest a weak molecular-orientation dependence for this site, evidenced by the fact that the nanoterrace site is the minimum energy binding site for C1, C2, and C3 (along the 2× direction only) molecules. Lacking the confining influence of a trench site, the nanoterrace site is consistent with broadening and switching of C1 to the 2× direction. The angular distributions indicate that C3 for the Ga-rich case must originate from two sites: one that orients the CH₃Br along the 2× direction and the other along the 4×. In the latter case, calculations indicate a site in the shallow trenches running along the 4× direction. Of course, the site assignments for the Ga-rich surface are made with the caveat that the structure of this surface remains in question [5,6].

An alternative explanation for the multiplicity of reaction channels could be substrate disorder. However, the similarity in intensities among the three channels in our measurements indicates that they originate from sites that are roughly equal in population, arguing in favor of their assignment to dissociation of molecules at regularly occurring lattice sites.

We have not addressed one important feature of these observations, viz. the partitioning of fragments into multiple energetic channels. Energetics are not easily calculated. However, we have used our electrostatic model to estimate the degree of ion stabilization at the specific sites discussed above. Correlation between our measurements and this model suggests that, as the interaction of the anion resonance with the substrate increases, the kinetic energies of the fragments first increase (as the ion separation time is decreased [15]) and then decrease (as the ion lifetime is shortened [16]). Wavelength-dependence TOF measurements for the Ga-rich surface (data not shown) are consistent with the affinity levels for the different channels being shifted by different amounts at different sites and reveal behavior consistent with a decrease in fragment kinetic energy with increasing stabilization energy in the strong-stabilization limit.

Our energy-resolved angular-distribution measurements show for the first time adsorption-site specificity in the kinetic energy release following a surface electron-transfer reaction. Electrostatic modeling of the molecular adsorption sites supports the idea that the multiple channels result from dissociation of molecules adsorbed at different sites, each with its own characteristic molecular orientation and perturbation of the molecular affinity level. Our observation of changes in the reaction dynamics with changes in substrate reconstruction and correlation of these changes with specific adsorption sites is distinct from our earlier work [1] and related electron-stimulated desorption-ion angular distribution measurements, and opens up an interesting area for exploration in the broader context of molecule-surface interactions.

We acknowledge support of this work by the NSF (No. DMR 99-03704) and the DOE (No. DE-FG02-90ER14104) and discussions with M. Wolf and D. Mocuta.

*Corresponding author.

Email address: nicholas@bnl.gov

†Current address: Chemistry Department, Brookhaven National Laboratory, Upton, NY 11973.

- [1] (a) P.H. Lu, P.J. Lasky, Q. Y. Yang, and R. M. Osgood, Jr., *Chem. Phys.* **205**, 143 (1996); (b) Q. Y. Yang *et al.*, *Phys. Rev. Lett.* **72**, 3068 (1994); (c) T. G. Lee, W. Liu, and J. C. Polanyi, *Surf. Sci.* **426**, 173 (1999); (d) H. Hirayama, A. Demeijere, and E. Hasselbrink, *Surf. Sci.* **287**, 160 (1993).
- [2] E. B. D. Bourdon *et al.*, *Faraday Discuss. Chem. Soc.* **82**, 343 (1986).
- [3] M. Jacoby, *Chem. Eng. News* **77**, No. 18, 46 (1999).
- [4] (a) P.R. Varekamp *et al.*, *Phys. Rev. B* **54**, 2101 (1996); (b) W. K. Wang, W. C. Simpson, and J. A. Yarmoff, *Phys. Rev. Lett.* **81**, 1465 (1998).
- [5] (a) J. E. Northrup and S. Froyen, *Phys. Rev. Lett.* **71**, 2276 (1993); (b) J. E. Northrup and S. Froyen, *Mater. Sci. Eng. B* **30**, 81 (1995); (c) W. G. Schmidt and F. Bechstedt, *Surf. Sci.* **360**, L473 (1996).
- [6] S.-H. Lee, W. Moritz, and M. Scheffler, *Phys. Rev. Lett.* **85**, 3890 (2000).
- [7] (a) C. Mailhot, C. B. Duke, and D. J. Chadi, *Surf. Sci.* **149**, 366 (1985); (b) R. J. Meyer *et al.*, *Phys. Rev. B* **19**, 5194 (1979).
- [8] (a) K. A. Khan *et al.*, *J. Phys. Chem. B* **103**, 5530 (1999); (b) N. Camillone III *et al.*, *J. Chem. Phys.* **109**, 8045 (1998).
- [9] P. H. Lu *et al.*, *J. Chem. Phys.* **101**, 10 145 (1994).
- [10] S. Black *et al.*, *Surf. Sci.* **382**, 154 (1997).
- [11] A. P. Mowbray, R. G. Jones, and C. F. McConville, *J. Chem. Soc. Faraday Trans.* **87**, 3259 (1991).
- [12] K. A. Khan *et al.*, *Surf. Sci.* **458**, 53 (2000).
- [13] K. A. Khan *et al.*, *J. Phys. Chem. B* **101**, 9077 (1997).
- [14] X.-Y. Zhu, *Annu. Rev. Phys. Chem.* **45**, 113 (1994), and references therein.
- [15] P. Ayotte *et al.*, *J. Chem. Phys.* **106**, 749 (1997).
- [16] P. J. Rous, *Phys. Rev. Lett.* **74**, 1835 (1995).